Technical Notes

TECHNICAL NOTES are short manuscripts describing new developments or important results of a preliminary nature. These Notes cannot exceed 6 manuscript pages and 3 figures; a page of text may be substituted for a figure and vice versa. After informal review by the editors, they may be published within a few months of the date of receipt. Style requirements are the same as for regular contributions (see inside back cover).

Computations of Transonic Turbulent Flow Past Airfoils Using Multigrid/Bi-CGSTAB Algorithm

Herng Lin*
Chung Shan Institute of Technology,
Lung-Tan 32500, Taiwan, Republic of China
and
Ching-Chang Chieng†
National Tsing Hua University,
Hsinchu 30043, Taiwan, Republic of China

Introduction

IN recent years, numerical predictions of transonic flow properties around an airfoil have been performed using various schemes.[1] Finding the airfoil shape for minimum drag or maximum lift/drag at a given operating condition is important in aerodynamic design. Accurate and rapid prediction of the flowfield can help in the optimal design of airfoils. Developing an accurate, robust, and efficient numerical scheme is the main object of this study.

The difficulty in achieving convergence in complex turbulent flow computation by employing a second-order closure model is well known. The slow convergence rate encountered is related to strongly nonlinear flow phenomena. In recent years, the convergence can be greatly improved and accelerated by using the conjugate gradient (CG) method[1] with a preconditioner, for example, variant bi-CG methods such as the biconjugate gradient stable (Bi-CGSTAB) method by Vorst[2] and the incomplete lower-upper factorization (ILU)[3] as the preconditioner to improve the rate of convergence in the previous study.[4] In the interim, a completely different approach, the multigrid method, has emerged for structured[5] and unstructured[6] grids as a particularly efficient technique for accelerating the convergence of numerical calculations. In the present work, the multigrid method of the fully approximation scheme by Jameson and Baker[7] and Jameson and Yoon[8] is adopted to remove the low-frequency errors as well as the high frequencies, so that the convergence can be sped up.

In this Note, the preconditioned Bi-CGSTAB relaxation method with ILU preconditioner is implemented to the compressible Navier–Stokes (N–S) solver with the Baldwin–Barth one-equation model[9] of turbulence. The present solver demonstrates efficient and fast convergence behavior if the multigrid and implicit algorithm are implemented simultaneously. Two-dimensional transonic turbulent flows over RAE2822 and Cast 7 airfoils are the test cases.

Governing Equations

The differential equations to describe the flow are the time-dependent, mass-averaged N–S equations plus the turbulence equation of the pointwise Baldwin–Barth model[9] for two-dimensional compressible flow. The resulting nondimensional equations in conservation law form can be formulated in curvilinear coordinates as follows:

$$\frac{\partial \hat{Q}}{\partial t} + \frac{\partial \hat{E}}{\partial \xi} + \frac{\partial \hat{F}}{\partial \eta} = \frac{\partial \hat{M}}{\partial \xi} + \frac{\partial \hat{N}}{\partial \eta} + \hat{H} \tag{1}$$

where matrices $\hat{Q}$, $\hat{E}$, $\hat{F}$, $\hat{M}$, $\hat{N}$, and $\hat{H}$ are made up of 5×1 column matrices; the elements of $\hat{Q}$ are $(1/J)\,[\rho, \rho u, \rho v, E_t, \Re]^T$; and the elements of source term $\hat{H}$ are $(1/J)\,[0, 0, 0, 0, H_5]^T$. The variable $\Re$ for the turbulence model is defined by k^2/ϵ, where k is turbulent kinetic energy and ϵ is the dissipation rate of k. The details of the other terms in the equations can be found in Ref. 9.

Numerical Algorithm

Spatial Differencing

The finite volume approach is used to formulate the difference equations in fully implicit form. Total variation diminishing (TVD) numerical flux[10] is applied for the convective term $\hat{E}$ and $\hat{F}$, and the central difference approximation is used for the viscous terms $\hat{M}$ and $\hat{N}$ and the Laplacian term of element H_5, where[9]

$$H_5 = (C_{\epsilon 2} f_2 - C_{\epsilon 1})(\Re \boldsymbol{P})^{\frac{1}{2}} + \left(\frac{M_\infty}{Re_\infty J \rho}\right)\left(\mu_\ell + \frac{2\mu_t}{\sigma_\epsilon}\right)\nabla^2 \Re$$

Time Integration

The implicit, unfactored, backward Euler scheme is employed for time advancement.[4] Upwind differencing in the ξ and η directions for the full N–S equations and the transport equation for variable $\Re$ is used. In the present study, the space-varying time step is employed to accelerate the convergence.[4]

Source Term Linearization

The source term $\hat{H}$ in Eq. (1) can be very large and cause the difference form of Eq. (1) stiff. To mitigate the stiffness, the source terms are treated implicitly. Refer to Ref. 11 for the procedures in deriving the source term Jacobian matrix $\hat{G}$ $(\equiv \partial \hat{H}/\partial \hat{Q})$. To improve stability, only negative source terms are linearized. Unfortunately, the production source term is positive, and so its linearization is not proper. Therefore, the strong coupling between the flowfield and the source term is linearized by the following pseudolinearization[12]:

$$\frac{\partial H_5}{\partial \Re} \sim -\frac{|H_{5\boldsymbol{P}}|}{(\Delta\, \Re)_{\max}}$$

where $H_{5\boldsymbol{P}}$ is the production part of H_5 and $(\Delta\, \Re)_{\max}$ is defined as $0.1\Re$, which is the estimated value of maximum variation for each iteration step.

Bi-CGSTAB Method

The unfactored matrix equations can be replaced by the nonfactored form, and the difference equations form a block pentadiagonal matrix system of equations. The algorithm of the Bi-CGSTAB method with ILU as a preconditioner is applied in the present work and is described in detail in Ref. 4.

Multigrid Formulation

In this study, a standard three- or four-grid-level saw-toothed and W-type multigrid cycle with fixed one-iteration strategy for

Received Feb. 28, 1997; revision received Aug. 15, 1998; accepted for publication Aug. 21, 1998.

*Research Scientist, Aerodynamics Branch, P.O. Box 90008-15-5.
†Professor, Department of Engineering and System Science. Senior Member AIAA.

switching from one grid level to another is adopted. Furthermore, the strategy of Ref. 5 is necessary for high-Reynolds-number viscous flow calculation because the grid size near the wall is very small and stretching rapidly. The detailed multigrid algorithm can be found in Refs. 5, 7, and 8. Three approaches using the multigrid formulation for coarse-grid calculation are under consideration. 1) The N–S equations are solved on the finest grid, whereas only the Euler fluxes are evaluated on the coarse grid.[13] 2) Full N–S equations are solved for all grid levels, but the transport equations for turbulent variables, i.e., $\Re$, k, and ϵ, are solved only for the finest grid level, and the needed eddy viscosity μ_t in the coarse-grid levels are collected from the finest grid.[12] 3) Full N–S equations and the transport equations for turbulent variables are solved for all grid levels. A relaxation procedure for damping the coarse-grid correction of the turbulent quantities must be employed.[14] A procedure similar to the work of Dick and Steelant[14] for turbulent quantity $\Re$ is given by

$$\Re_{\text{new}} = \frac{\Re_{\text{old}} + \alpha\delta\Re^{+}}{\Re_{\text{old}} - \alpha\delta\Re^{-}}\Re_{\text{old}}$$

where $\Re^{+}$ and $\Re^{-}$ are the positive and negative coarse-grid correction, respectively. The relaxation factor α is selected as 0.3.

Testing Problems and Boundary/Initial Conditions

Numerical computations have been performed for 1) two-dimensional transonic flow past a subcritical airfoil RAE2822 at 3.19-deg angle of attack for the freestream condition $M_\infty = 0.73$ and $Re_\infty = 6.5 \times 10^6$ and 2) two-dimensional transonic flow past a supercritical Cast 7 airfoil within the range from -2- to 5-deg angle of attack for the freestream condition $M_\infty = 0.7$ and $Re_\infty = 6 \times 10^6$. Two O-type grids are generated by the hyperbolic grid-generation scheme. The grid system for the RAE2822 airfoil is a 169×73 grid, with 81 points on the upper surface, 81 points on the lower surface, and 8 points on the blunt trailing edge, i.e., base region. The grid system for the Cast 7 airfoil is a 137×73 grid, with 65 points on the upper and lower surfaces and 8 points on the blunt trailing edge. The grid points in the normal direction are exponentially stretched away from the wall, and the first grid line is at a distance of 7×10^{-6} chord lengths from the wall. The boundary of the computational mesh extends 25 chord lengths in the normal direction. At the $\xi = 1$ and $\xi_{\max}$ boundaries, the periodic boundary condition is employed. The overlapped interface flux was treated specially to sustain second-order accuracy. At the $\eta = \eta_{\max}$ boundary, a subsonic inflow/outflow condition is specified. The characteristic extrapolating technique is applied. At the $\eta = 1$ boundary, no-slip conditions and zero normal pressure and concentration gradient are imposed

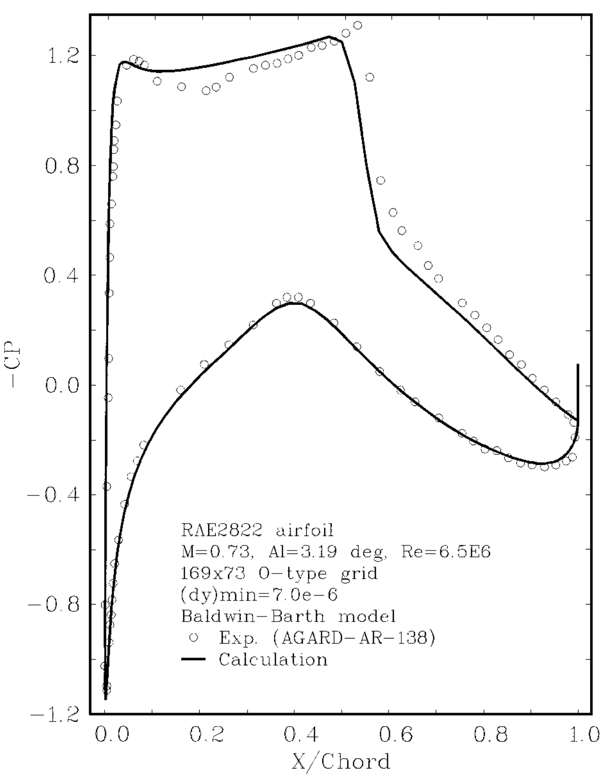

Fig. 1 Computed and experimental surface pressure distributions for RAE2822 airfoil; $M_\infty = 0.73$, $\alpha = 0$ deg, $Re_\infty = 6.5 \times 10^6$.

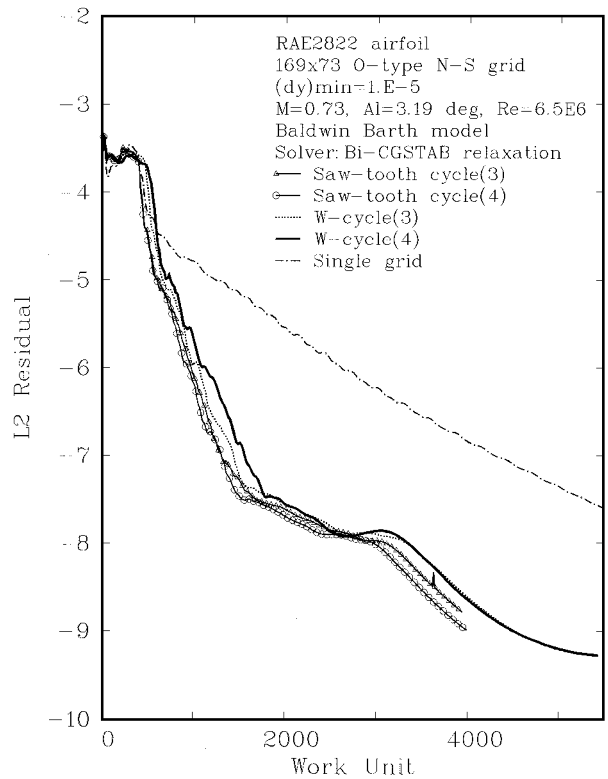

Fig. 2 Convergent histories for different multigrid sequences.

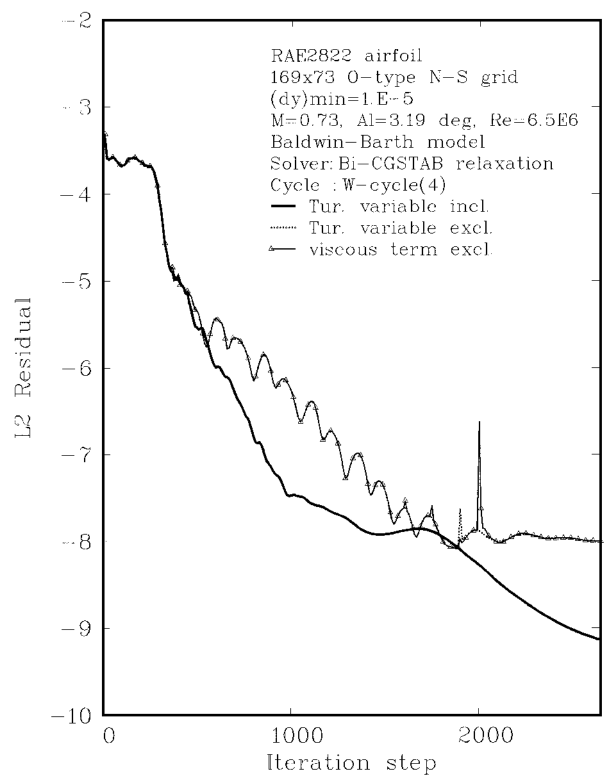

Fig. 3 Convergent histories for different coarser-grid calculations.

on the wall. The eddy viscosity μ_t and $\Re$ vanish at the solid wall. A uniform flowfield is chosen as the initial condition for mean flow equations. A uniform value of $\Re_{\text{int}} \sim 1000$ is set as the initial guess.

Results and Discussion

The computed surface pressure distributions of the RAE2822 airfoils can be compared with experimental data of Ref. 15 (shown in Fig. 1). The convergence histories with different multigrid cycles are plotted in Fig. 2. The efficiency of the multigrid cycle is measured by the amount of computational effort required to reduce the residual to a given level. The computational effort is measured by work units, which are defined in terms of a single N–S calculation on the finest grid. Therefore, the work units required in a three-level saw-toothed cycle is estimated as $(1 + \frac{1}{4} + \frac{1}{16} + \frac{1}{64}) = 1.325$. The work units required in a four-level saw-toothed and three-level and four-level W-type cycles are 1.328125, 1.6250, and 1.8125, respectively. For this test case, the L_2 residuals calculated by the four different multigrid cycles are similar. The convergent speed using the W cycle is not higher than those using saw-toothed cycles at the same grid level. But the convergent efficiency with and without the multigrid cycle is apparent.

The convergence histories 1) with integrating the $\Re$ equation, 2) without integrating the $\Re$ equation, and 3) without integrating the $\Re$ equation and evaluating viscous flux for the coarser-grid calculation are compared in Fig. 3. Better multigrid performance is obtained with integrating $\Re$ equation for the damping factor $\alpha = 0.3$. Without solving the turbulence transport equation on the coarser grids, the convergence histories exhibit oscillation and are less good.

The convergence histories using different implicit schemes are plotted in Fig. 4. The lower-upper symmetric Gauss–Seidel (LU-SGS) scheme[16] and diagonally dominant alternating direction implicit (DDADI)[17] scheme are approximate factorization (AF) schemes but are low-factorization-error schemes if strong source terms exist.[18] Without multigrid acceleration, the Bi-CGSTAB relaxation method is the fastest and smoothest convergent scheme compared with the other AF schemes. Combined with the multigrid algorithm, the L_2 residuals using the DDADI scheme exhibit a similar convergent rate with the Bi-CGSTAB relaxation method and outperform the LU-SGS scheme. The comparison demonstrates that the Bi-CGSTAB relaxation scheme is the best in terms of convergence characteristic if multigrid cycle is not applied but does not outperform the DDADI method when the multigrid algorithm is combined.

A second test was performed for transonic turbulent flow past a Cast 7 airfoil for freestream Mach number 0.7 and freestream Reynolds number 6×10^6 with angle of attack ranging from -2 to 5 deg. The computed lift and drag coefficients and surface pressure distributions can be compared with experimental data of Ref. 19. The corrected angle of attack $\Delta\alpha$ is assumed -0.35 deg for all of the cases. The computed surface pressure coefficient distributions are in good agreement with the Aircraft Research Association experimental data below 3-deg angle of attack and are different for the cases of 4- and 5-deg angle of attack. The lift coefficient C_L vs angle of attack is plotted in Fig. 5. The C_L predictions are good if the angle of attack is less than 4 deg. The calculated stall angle is correct. The C_D predictions are underestimated as compared with the experimental data if the angle of attack is more than 4 deg. The experimental data suggest that the stall angle of the Cast 7 airfoil is near 4.5-deg angle of attack, and the present turbulence model need to be modified for predicting large separation phenomena. The convergent histories for the cases of angles of attack ranging from -2 to 5 deg are similar to the first case. The L_2 residual for these calculations can be reduced to six orders within 1500, 1550, 1850, and 2000 iterations, respectively, and the lift/drag coefficients are fully converged.

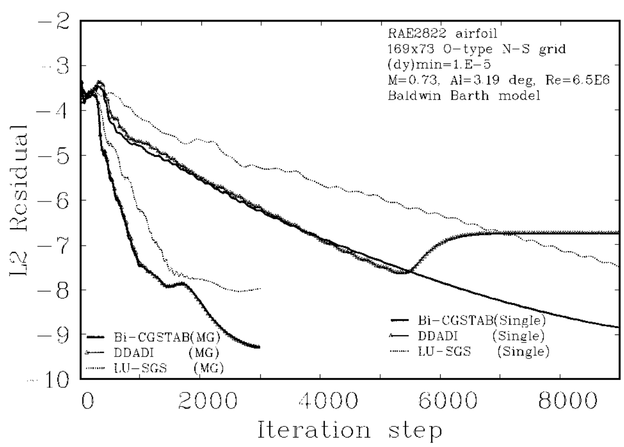

Fig. 4 Convergent histories for different implicit methods.

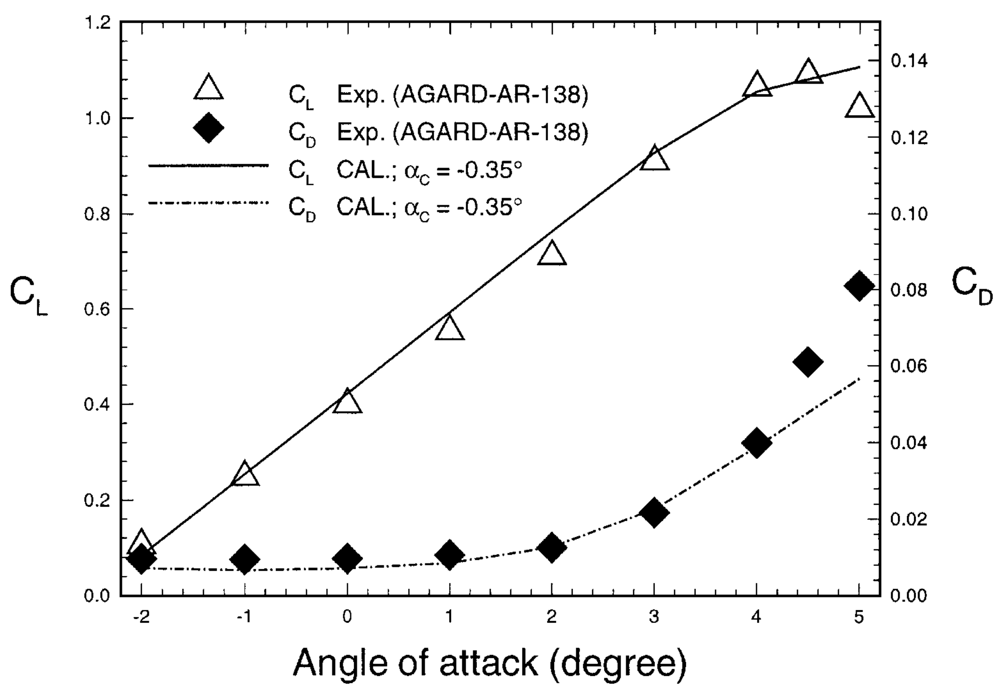

Fig. 5 Computed and experimental lift/drag coefficients vs angle of attack for Cast 7 airfoil; $M_\infty = 0.7$, $Re_\infty = 6 \times 10^6$.

Conclusion

A numerical model solving the full N–S equation with the Baldwin–Barth one-equation model of turbulence is satisfactorily developed. This numerical method is based on a finite volume, TVD spatial discretization and is integrated by an implicit unfactored method with preconditioning Bi-CGSTAB algorithm matrix solvers with multigrid acceleration. The test cases demonstrate good lift/drag predictive capability, as well as the efficiency and robustness of the convergence for transonic turbulent flow past a RAE2822 subcritical airfoil and a Cast 7 supercritical airfoil.

Acknowledgment

The authors thank the National Science Council of the Republic of China for support under Contract NCHC85-04-014.

References

[1]Hestenes, M. R., and Stiefel, E., "Methods of Conjugate Gradients for Solving Linear Systems," *Journal of Research of the National Bureau of Standards*, Vol. 49, No. 6, 1952, pp. 409–436.

[2]Van der Vorst, H. A., "Bi-CGSTAB: A Fast and Smoothly Convergent Varient of Bi-CG for the Solution of Nonsymmetric Linear Systems," *SIAM Journal on Scientific and Statistical Computing*, Vol. 13, No. 2, 1992, pp. 631–644.

[3]Meijerink, T. A., and van der Vorst, H. A., "Guidelines for the Usage of Incomplete Decompositions in Solving Sets of Linear Equations as They Occur in Practical Problems," *Journal of Computational Physics*, Vol. 44, No. 1, 1981, pp. 134–155.

[4]Lin, H., Yang, D. Y., and Chieng, C. C., "Variants of Biconjugate Gradient Method for Compressible Navier–Stokes Solver," *AIAA Journal*, Vol. 33, No. 7, 1995, pp. 1177–1184.

[5]Thomas, J. L., Taylor, S. L., and Anderson, W. K., "Navier–Stokes Computations of Vortical Flows over Low Aspect Ratio Wings," AIAA Paper 87-0207, Jan. 1987.

[6]Anderson, W. K., Rausch, R. D., and Bonhaus, D. L., "Implicit/Multigrid Algorithms for Incompressible Turbulent Flows on Unstructured Grids," *Journal of Computational Physics*, Vol. 128, No. 2, 1996, pp. 391–408.

[7]Jameson, A., and Baker, T. J., "Multigrid Solution of the Euler Equations for Aircraft Configurations," AIAA Paper 84-0093, Jan. 1984.

[8]Jameson, A., and Yoon, S., "Multigrid Solution of the Euler Equations Using Implicit Schemes," *AIAA Journal*, Vol. 24, No. 11, 1986, pp. 1737–1743.

[9]Goldberg, U. C., and Ramakrishnan, S. V., "A Pointwise Version of Baldwin–Barth Turbulence Model," *Computational Fluid Dynamics*, Vol. 1, 1993, pp. 321–328.

[10]Yee, H. C., and Harten, A., "Implicit TVD Schemes for Hyperbolic Conservation Laws in Curvilinear Coordinate," AIAA Paper 85-1513, July 1985.

[11]Sahu, J., and Danberg, J. E., "Navier–Stokes Computations of Transonic Flows with a Two-Equation Turbulence Model," *AIAA Journal*, Vol. 24, No. 11, 1986, pp. 1744–1751.

[12]Siikonen, T., "An Application of Roe's Flux-Difference Splitting for k–ϵ Turbulence Model," *International Journal for Numerical Methods in Fluids*, Vol. 21, No. 11, 1995, pp. 1017–1039.

[13]Yokota, J., "A Diagonally Inverted LU Implicit Multigrid Scheme for the 3-D Navier–Stokes Equations and a Two Equation Model of Turbulence," AIAA Paper 89-0467, Jan. 1989.

[14]Dick, E., and Steelant, J., "Multigrid Solution of the Steady Compressible Navier–Stokes Equations Coupled to the k–ϵ Turbulence Equations," AIAA Paper 95-1669, June 1995.

[15]Cook, P. H., McDonald, M. A., and Firmin, M. C. P., "Aerofoil RAE2822-Pressure Distributions, and Boundary Layer and Wake Measurement," AGARD-AR-138, Rept. A6, May 1979.

[16]Shuen, J. S., and Yoon, S., "Numerical Study of Chemically Reacting Flows Using Lower–Upper Symmetric Successive Overrelaxation Scheme," *AIAA Journal*, Vol. 27, No. 12, 1989, pp. 1752–1760.

[17]Schroder, W., and Hartman, G., "Implicit Solutions of Three-Dimensional Viscous Hypersonic Flows," *Computers and Fluids Journal*, Vol. 21, No. 1, 1992, pp. 109–132.

[18]Shih, T. I.-P., "Approximate Factorization with Source Terms," *AIAA Journal*, Vol. 29, No. 10, 1991, pp. 1759, 1760.

[19]Stanewsky, E., Puffert, W., Muller, R., and Bateman, T. E. B., "Supercritical Airfoil Cast 7—Surface Pressure, Wake and Boundary Layer Measurements," Aircraft Research Association, Bedford, England, UK, AGARD-AR-138, Rept. A3, May 1979.

J. Kallinderis
Associate Editor

Blockwise Adaptive Grids with Multigrid Acceleration for Compressible Flow

Lars Ferm*
Uppsala University, S-75104 Uppsala, Sweden
and
Per Lötstedt†
Saab AB, S-58188 Linköping, Sweden

Introduction

IN most programs in practical use for flow calculation, e.g., around an airplane, the grid is partitioned into a number of blocks with a structured grid in each block. The data structure of a multiblock grid allows for a finer grid in certain blocks and a coarser grid in other blocks. With refinement and coarsening of the grid, it is possible to concentrate the cells in areas where they are needed to obtain sufficient accuracy in the final solution.

Adaptive grid procedures for structured grids are developed in Refs. 1–4. Either new cells are introduced into the grid or the available cells are moved to the region where the resolution is poor. The decision of where to change the grid density is based on estimates of the solution error or the truncation error or on a sensor that detects a feature of the flow requiring a finer grid, such as a shock. With a better distribution of the cells, the same solution accuracy is obtained with fewer cells. Memory is saved, and the CPU time is shorter.

The convergence rate to steady state is often improved dramatically by using a multigrid method.[5,6] In practice, the number of levels in complicated multiblock grids is limited to three or four.

Here we combine adaptive grid refinement and coarsening with the multigrid algorithm for efficient calculation of the steady-state solution and apply the method to the Euler equations. All of the cells in a block are refined or coarsened. In this way, no new data structure is introduced, but the total number of cells will sometimes be greater than necessary.

Numerical Solution and Adaptation

The Euler equations are discretized on a structured grid with a cell-centered finite volume method according to Jameson.[7] The grid is partitioned into blocks. Grid refinement in a block is always made by halving h, and coarsening always means doubling h in all three directions of the grid. At the block faces, two extra layers of ghost cells are added to simplify the evaluation of the difference stencil in the cells adjacent to the face, as is usual in multiblock codes. The values in the cells in the overlapping region are determined by the boundary conditions, or there is a neighboring block with cells corresponding to those in the extra layers. In the latter case, the values in the ghost cells are given by the values in the adjacent block. For the solution to remain reasonably accurate and stable also at the block boundary, a ghost cell in the coarser grid occupies the same volume as eight cells in three dimensions in the finer grid. This implies that the grid size is at most doubled between two blocks.

There are two cases at a block interface. The cell face at the boundary in one block coincides with a cell face in the other block. Then the solution values in the ghost cells are copied from the values in the corresponding inner cells in the other block. If a coarse grid is adjacent to a fine grid, then the values in the ghost cells in the coarse grid are computed by a volume-weighted average. In the fine grid, the conservative variables are calculated by trilinear interpolation.

These transfers of the solution between the grids will not make the scheme conservative, and problems may occur if a shock crosses

Received Jan. 16, 1996; revision received Aug. 5, 1998; accepted for publication Aug. 21, 1998.

*Research Scientist, Department of Scientific Computing, P.O. Box 120.
†Specialist, Aerodynamics Department.